NANOSTRUCTURAL CHARACTERIZATION OF GLUTATHIONE-S-TRANSFERASE IMMOBILIZING CHITOSAN MODIFIED SCREEN PRINTED CARBON ELECTRODE BY ATOMIC FORCE MICROSCOPY

Buddhapala Wongkaew[1], *Porntip Wongkaew[2], Panupong Thanutong[1] and ChitsanuphongThanutong[3]

[1]Metropolitan Waterworks Authority, Bangkok 10210; [2]Faculty of Agriculture, Khon Kaen University, KhonKaen 40002; [3]Ministry of Digital Economy and Society, Bangkok 10210, Thailand.

ABSTRACT: Immobilization of a bio-recognition element to the surface of a functional working electrode is fundamental for effective biosensor development. In this study, the enzyme glutathione-s-transferase (GST) that constitutes a protein superfamily involving various distinct chemical transformations was introduces as a versatile tool for the sensing of environmental toxicants. Functional electrode surface was made by self-assembly of a great bioscaffold chitosan onto screen-printed carbon electrode surface concerning to its excellent covalent bonding binding of biomolecules. To enhance the enzyme proximity, glutaraldehyde was employed as an assisting bifunctional cross-linker. The self assembled chitosan layer and the GST immobilizing nanostructural features were explored by morphological imaging and several quantitative analyses such as surface grain size and distribution, power spectrum density (PSD) algorithm, fractal dimension character and other important surface roughness parameters via atomic force microscopy (AFM). Vertical aggregation of the successive layer was clearly verified in all quantitative approaches. Exceedingly, a better understanding in the direction of aggregation along with the growth mechanism was obtained by PSD analysis and the fractal dimension values gained around 2.27 for modified chitosan surface and 2.02 for GST immobilized chitosan modified screen-printed carbon basement could thus imply for the diffusion limited model in this growth mechanism.

Keywords: Immobilization · Glutathione-s-transferase· Chitosan · Biosensor development · Atomic Force Microscopy

1. INTRODUCTION

Recently, researchers based on electrochemical biosensor have been attractively considered as potential successors to the development of new methodologies for economical and real-time monitoring of environmental pollutants and also for prevention of toxic materials in the environment [1] The main functional activity belongs to the oxidising and reducing ability of the selective bio-recognition elements that make a high throughput screening of analytical target possible in a reliable manner within a fraction of seconds. Therefore a critical step for the development of biosensor is the selection of a proper bio-recognition element and the immobilization of this element to the surface of a working platform. Although there have been a wide range of bio-molecular recognition elements suggested, enzymes are historically the first molecular recognition elements included informer biosensors and continue to be the basis to date for newly biosensor development and application [2, 3]. Enzymes provide several advantages due to their excellent selectivity for the targeted substrate and high catalytic activity. In addition, a relatively high reaction rate with enzyme operation is commonly achieved at mild conditions of temperature, pressure, and pH which makes substantial process energy savings and reduced manufacturing costs. Moreover, they are natural substance being mostly biodegradable protein and peptides that can be easily withdrawn from the contaminated environment without disposal problems.

Immobilization of the enzymes onto suitable platforms is crucial for maintaining their catalytic activity and long-term stability, and also for biosensor development. Several techniques have been proposed for enzyme immobilization by physical and chemical covalent bonds interactions such as the method of entrapment, encapsulation, solid support and self-immobilization [4]. At present, many innovative enzyme immobilization techniques have been reported for several implementations including biosensor fabrication.

A commercial enzyme-based biosensor has also been generated especially in the case of glucose oxidase, lactate oxidase, urease and glutamate oxidase immobilization for a practical detection of glucose, lactate, urea, and glutamate, respectively [5]. In pesticide determination studies, the main enzymes used are acetylcholinesterase, butyrylcholinesterase, cholinesterase, acid phosphatase, ascorbate oxidase, acetolactate synthase, urease, aldehyde dehydrogenase and glutathione-s-transferase [5, 6]. On the other hand, it is necessary to choose a suitable platform that provides good support for demand in both catalytic and noncatalytic activities including productivity, rapidity, selectivity, separation, control, and down the streaming process. The supporting platform has to possess a large hydrophilic surface area, chemical and mechanical stability, and antimicrobial attack. Many types of constructed nanomaterials such as nanoparticles, nanofibers, nanotubes, mesoporous silica, and nanometals have been suggested due to their extremely high surface area-to-volume ratios for a great enhance the immobilization. But a lot of complications have been arisen because of their dispersion difficulty in reaction solutions and subsequent processes, besides their cost are incredibly high. A natural material chitosan is another nano-matrix choice in our attention because of its biocompatibility altogether with its prompt availability and inexpensive productivity which allows a wide array of application in environmental engineering. It is the partially deacetylated form of an environmental friendly chitin [poly (N-acetyl-D-glucosamine)], the main exoskeleton component of crustaceans and cell wall of fungi that are the second most abundant polysaccharide in nature after cellulose. Chitosan is considered to be an excellent bioscaffold by virtue of many interesting properties related to both biological and electrochemical affinity [7, 8]. It is indeed a natural cationic biopolymer containing robust reactive functional groups (–OH and –NH2) for ionic or covalent bonding binding of biomolecules such as DNA and proteinaceous enzymes and for other chemical modifications as well. As it is soluble in weak acids and forms quite stable hydrogel film which make it suitable matrix for various micro-fabrications. Our previous study on the modification of a screen printed carbon electrode by surface incorporation with chitosan has demonstrated one among potent application for obtaining an effective and affordable electrochemical implement [1]. With reference to such excellent advantages, it was further used to achieve another successful immobilization of enzyme in this present work to gain an effective specific biosensor.

According to the recent advance in nanotechnological science, many more sophisticated techniques have been developed for the analysis of interfacial events at micro and nanoscale. Among various instrumentations that enable imaging, atomic force microscopy (AFM) is the only empower technique for material surface visualizing at sub-nanometer accuracy. In comparison to standard scanning (SEM) and transmission electron (TEM) microscopy, the AFM not only offers the capacity to visualize nanometric features in two and three dimensions but also the physicochemical characteristics including its spatial distribution mapping of surfaces and the permittivity to perform an observation in several environments for example in air, vacuum and liquid environments with little or even no sample preparation requirement. The correlation between the physicochemical properties of biomaterials and the resulting biological response can also be resolved significantly. Inferably, the AFM allows superlative tool for imaging, quantifying, manipulating and other analyses of inspection materials at nanometer level without perturbation of the native characteristics. The fact that nano-topographical surfaces influence charge density and electric field strength, quantitative characterization of surface morphology is thus very important. To date, AFM has been employed progressively for exploring the surface morphological features especially in the research area of surface engineering [1, 9].

In the present study, an enzyme glutathione-s-transferase (GST) was chosen as a model for immobilization. GST is one of the major detoxifying enzymes widely distributed in animals, plants, and microorganisms that actives against oxidative stress and toxic electrophiles substances [10]. Its notify activity in several types of chemical transformations has led to a great potency in biotechnological applications including in the field of bioremediation, elimination of environmental toxic compounds and biosensor preparation [11, 12]. A biopolymer chitosan was selected as an appropriate platform for the GST immobilization and a disposable strip of screen-printed carbon electrode (SPCE) was used as a solid basement for surface modification with the chitosan by self-assembled deposition method according to our previous report [2]. Subsequently, a bifunctional cross-linker, glutaraldehyde (GA) was used for cross-linking and activating the –NH$_2$ group of chitosan scaffold to ensured good biocatalyst activity and stability [4]. The accomplishment of this immobilization event was then deeply evaluated through high-resolution AFM imaging and important interfacial parameters analyses.

2. MATERIALS AND METHODS

3.

2.1 Materials

Chitosan (85% degree of deacetylation) with a molecular weight of 0.28 kDa was obtained from Bioline Lab, Co., Thailand. Glutathione-S-transferase (GST, EC 2.5.1.18) lyophilized powder from the equine liver with a specific activity of ≥25 units/mg protein was purchased from Sigma-Aldrich Co. LLC, USA. Other chemicals for experimental reagent preparation were bought from Ajax Finechem Pty, Ltd., Australia. All the chemicals were of analytical grade and used as received. Solutions and reagents were prepared using high purity deionized water of 18.2 MΩ from Milli-Q RG system (Millipore Corporation, MA, USA.). Screen printed carbon electrode DRP-150 was provided by DropSens, ParqueTecnológico de Asturias, S.L.Llanera (Asturias) Spain.

2.2 Preparation of Chitosan Modified Electrode Platform Trials

Chitosan solution (1%, w/v) was done by dissolving 1 g chitosan in 100mL of 1% (v/v) acetic acid solvent and the solution was filtered to remove insoluble materials. A self-assembled monolayer of chitosan was formed on carbon working spot of screen-printed carbon electrode (SPCE) by applying a 3.0 μl drop of chitosan solution and naturally dried up at room temperature. The modified working surface was then fixed with a 10μl drop of 0.1 M NaOH for 30 min left it dried again prior to use.

2.3 Immobilization of GSTenzyme

To form a better support condition for enzyme immobilization, the chitosan modified working surface was to be activated by an incorporation of glutaraldehyde (GA) covalent attachment. This working surface spot was treated with a 5 μl drop of 2.5% glutaraldehyde for 30 minutes at room temperature and rinsed with deionized water afterward to remove an excess of its particle. Preparation of 3 U GST enzyme solution was done in 0.05 M PBE that formulated from 0.05 M Phosphate buffer saline at pH 6.5 containing 0.05 M EDTA and 0.1 M KCl [7]. Immobilization of GST was then performed by adding a 5 μl drop of this enzyme solution onto the GA-activated chitosan modified working surface and incubated at room temperature for 2 hours. It was then washed down inordinate molecules with deionized water.

2.4 AFM imaging and analysis

Nanostructure imaging of surface characteristics was carried out by an atomic force microscope model XE-120 (Park Systems Corp., Suwon, Korea) through a true non-contact mode. The observation was done in non-contact mode under ambient conditions with standard PPP-NCHR silicon cantilever consisting a < 10 nm tip radius (Nanosensors TM, Neuchâtel, Switzerland) with a spring constant of 42 N/m force constant and resonant frequency of 320 kHz. An x-y accessible $1 \times 1 \mu m$ area at 0.5 Hz scan rate was inspected with XEP software for data acquisition and XEI software for image processing and quantitative analysis of the surface topography. Important parameters such as an average roughness Ra (nm), root mean square or standard deviation of the height value Rq (nm), height different or peak-to-valley (Rpv), ten-point height (Rz), mean spacing average (Rsm), skewness (Rsk), kurtosis (Sku), power spectrum density (PSD) algorithm, fractal dimension and grain aggregation were then successively identified.

3. RESULTS AND DISCUSSION

3.1 AFM imaging of surface morphology

A creation of GST enzyme immobilization on working chitosan platform was sighted up by AFM imaging. Remarkable changing in surface morphology could be seen following the modification of screen-printed carbon spot area of the SPCE with chitosan and the immobilization of GST enzyme onto chitosan modified platform with the aid of GA bifunctional covalent as shown in Fig.1. Morphological feature at nanometer scale of the scanned surface within a projection area of $1 \times 1 \mu m$ has been revealed in 3D illustration for the screen printed carbon basement of SPCE in Fig. 1A, the chitosan modified SPCE (SPCE-Chi) in Fig.1B and the GST immobilized chitosan modified SPCE (SPCE-Chi-GST) in Fig.1C, respectively. The different feature appearance from each other among these obtaining images, thus, is likely an indication of a progress in the surface modification.
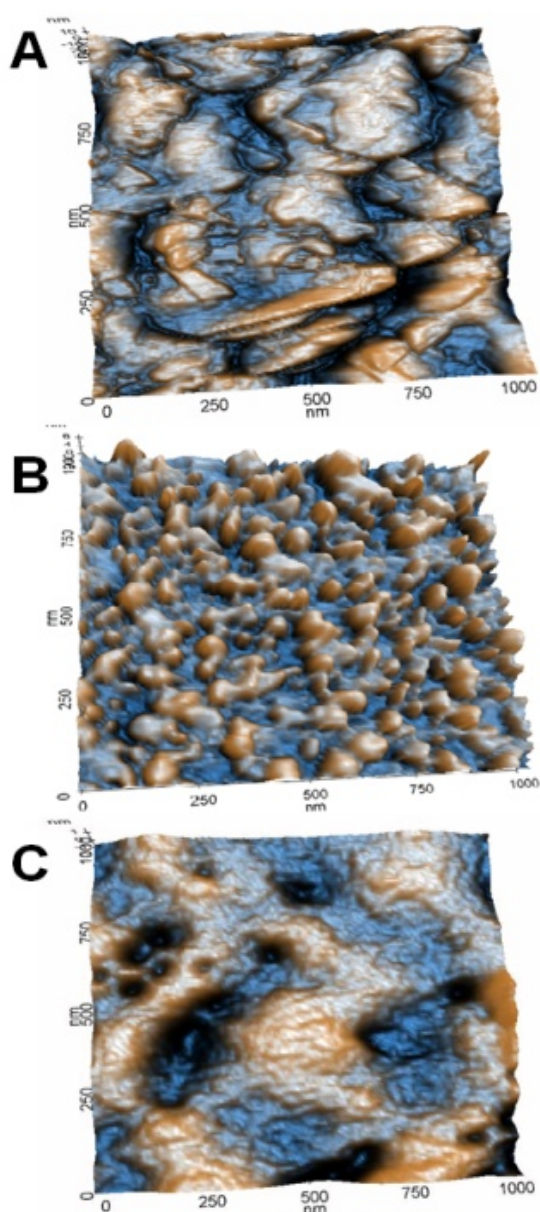
detected as grains by a watershed algorithm with a software-based image processing. In this observation, the XEI software of Park System was used in quantitative analysis of the surface grain profile to provide comparative information related to the success of SPCE modification with chitosan and GST immobilization onto chitosan modified SPCE. Table 1 presents the measured surface grain information in an average of grain area, volume, perimeter, and peak-to-valley via level 2.5 filter of the watershed algorithm by the XEI software. Differences among the surface natures could be demonstrated in this grain size quantification. Much larger in the area, length, and perimeter but smaller in volume and peak-to-valley value of the grains from SPCE-Chi and SPCE-Chi-GST than the original SPCE surface were obtained in this determination. With reference to these values, the surface looks after chitosan modification and GST immobilization became rather slightly wrinkle taper smear on top of screen-printed carbon basement in consent to our previous report [2].

Table1 Surface grain structure estimation on a working platform of bare SPCE, SPCE-Chi, and SPCE-Chi-GST, at 1x1 µm AFM scan size.

Parameters		Bare SPCE	SPCE-Chi	SPCE-Chi-GST
Area (nm^2)	Mean	2.215	4.185	3.165
	Std.	3.385	1.029	3.792
Volume (nm^3)	Mean	1.882	0.037	1.063
	Std.	2.943	0.089	1.307
Length (nm)	Mean	67.544	83.854	89.109
	Std.	43.259	82.999	64.534
Perimeter (nm)	Mean	205	273	252
	Std.	155	335	179
Rpv (nm)	Mean	10.212	6.942	5.683
	Std.	5.995	3.164	3.777

Note: SPCE = screen printed carbon electrode, SPCE-Chi = chitosan modified screen printed carbon electrode, SPCE-Chi-ActC = activated carbon blending chitosan modified screen printed carbon electrode, *Rpv* = peak-to-valley, Std = root mean square or standard deviation

Fig. 1 Three-dimensional AFM nanoscale surface images of (A) bare screen printed carbon spot area of a SPCE, (B) chitosan modified screen printed carbon spot and (C) chitosan modified screen printed carbon spot after immobilization with glutathione-s-transferase.

3.2 Surface grain profile

As the AFM nanostructure images have shown a wavy surface texture containing various ripples against a background. These ripples can be

Statistical information on groups of these grains could also be evaluated to define the distribution of the grain size. Quantitative scoring for the grain size distribution through histogram plots is shown in Fig. 2. Distinction in grain size

distribution is also manifested among these surfaces, thus exemplify asymmetric growth evidence following chitosan deposition and GST immobilization process.
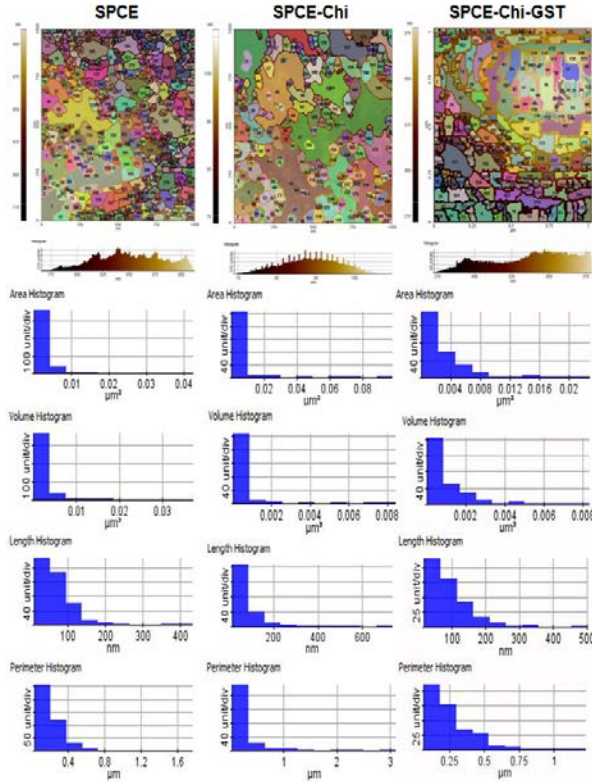

Fig. 2   Grain size distribution histogram on working surface of SPCE, SPCE-Chi, and SPCE-Chi-GST at 1x1 µm AFM scan size:

3.3 Power spectrum density (PSD) and fractality

Further analysis of surface feature was performed by power spectral density (PSD) which is one of the important parameters in surface roughness representation. PSD of the loaded image is obtained from Fourier Transform (FT) of the image and reflects the root mean square (*Rq*) roughness of the sample surface. It is equal to the square of FT and RMS roughness value squared according to the relation: $PSD = FT^2 = Rq^2$. Information given from PSD graph provides not only roughness status but also the contribution of each frequency components to the total roughness of the surface [13]. The curves depicted in Fig. 3 show the PSD function of the waveguide evaluated along a line in the AFM image of each working surface acquired via 1x1 µm scan size. The contribution of each spatial frequency to the line profile versus frequency is represented. The most

outstanding peak with the highest frequency intensity in each curve at 2, 3 and 1 µm⁻¹ was delivered from SPCE, SPCE-Chi, and SPCE-Chi-GST working surface, respectively. In spite of these low spatial values, the curves indicate that the spatial periodicity of resisting molecular aggregates existed in the surfaces is varied following the modification with chitosan and the immobilization with GST.
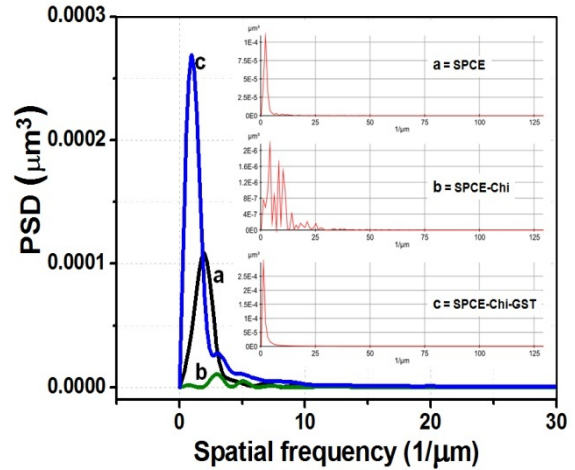

Fig. 3   Power spectral density (PSD) function of the waveguide analyzed along a line in the AFM image of each working surface acquired via 1x1 µm scan size: (a) bare SPCE, (b) SPCE-Chi and (c) SPCE-Chi-GST.

Fig. 4 displays 2D isotropic power spectra in a log-log plot of PSD and frequency of each working surface in comparison to their relevant slopes for an estimation of the fractal dimension by triangulation method included in the XEI software. All the 2D PSD plots show quite similar in the slope pattern that gradually decreasing from lower to higher spatial frequencies but with a bit different in their waviness concerning to their relative waveguide profile in Fig. 3. These PSD plots also reflect the roughness contribution in their correlative surface. Moreover, a condensed description in term of the fractal dimension of the surface can be quantified based on this PSD function in a more sample-independent manner according to the inverse power law decay [14]. Generally, the fractal model provides more detail on rough surface morphology considering the concepts of scale and the symmetry elements. In another word, fractal objects can be characterized by morphological invariance under scale variance in a restricted range of the spatial scales and allow determination of surface morphology by scale laws [15]. The calculated fractal dimensions in this study are 2.12, 2.27 and 2.02 for SPCE, SPCE-Chi

and SPCE-Chi-GST working surface, respectively (Table 2), suggesting a small but markedly difference among each surface texture in subsequent to the layer-by-layer deposition process due to their distinct attribution in the fractal figure occupied along these investigated 3D images.

The higher value of fractal dimension in SPCE-Chi working surface represents a higher level of fractality and a more continuous irregular feature of the surface roughness than the others while the smaller value represents a smoother top surface [16]. The lowest value obtained in the case of SPCE-Chi-GST thus infers a smoothening flow of successive GST immobilization. This evidence also indicates a vertical growing of the filling GST on the basal chitosan modified screen-printed carbon surface.
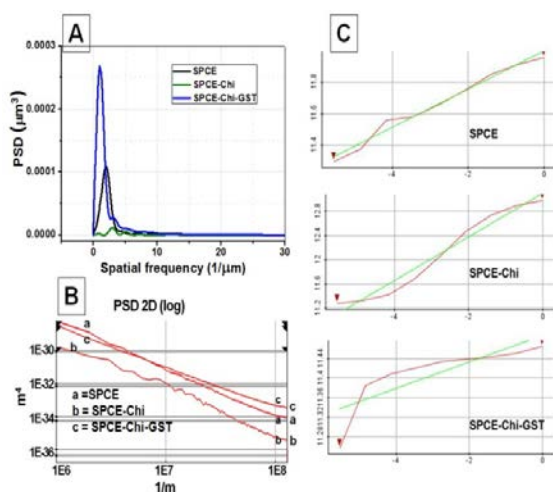

Fig. 4 Two dimensional (2D) isotropic power spectral plots of log PSD and frequency of the working surface of SPCE, SPCE-Chi and SPCE-Chi-GST at 1x1 μm AFM scan size in comparison to their relevant slopes for an estimation of the fractal dimension by a triangulation method.

3.4 Surface roughness characteristics

in comparison to a screen printed carbon basement layer was measured from the obtained AFM images by important statistical parameters such as average roughness (Ra), root mean square roughness (Rq), peak-to-valley (Rpv), ten-point height (Rz), mean spacing average (Rsm), skewness (Rsk), kurtosis (Rku), and mean spacing average (Rsm). Table 2 displays the estimated values which explicitly show trends in their layer by layer toping relation. The Ra and Rq similarly describe overall height distribution profile as a result of the mean height and the standard deviation of the profile height hence imply the top surface wavy roughness characteristics which

seem to remarkably increase over one order of magnitude in chitosan modified screen-printed carbon basement, SPCE-Chi, in consent to our previous report [2]. Simultaneously, these surface roughness parameters appear to be highest in the SPCE-Chi-GST working surface due to the succession of GST oriented assembling. The values gained in Rpv and Rz clearly explain a differentiation in spike depth among the figuring surface profiles that fluctuate from a high plateau of SPCE to a shallow top-up layer in SPCE-Chi and an up level of the dept again in the following SPCE-Chi-GST. In cases of the Rsk and Rku representing the shape and sharpness of the height distribution, on the other hand, the porosity and load carrying capacity, are decreased in SPCE-Chi from the value of the basal SPCE working surface thus suggesting a growing of valleys and cavities appropriate to groove the enzyme molecules. While an increasing of these value are scored on the working surface of SPCE-Chi-GST, on contrary, suggesting a growing of peaks rather than cavities by virtue of the fill-up GST immobilization process. Measurement of the Rsm shows values down from 0.39 μm in SPCE to 0.11 and 0.08 μm in SPCE-Chi and SPCE-Chi-GST. These values similarly indicate a decreasing of lateral adjacent peak spaces following a diffusive topping aggregation in the corresponding stepwise manipulation. All the parameters determined thus definitely assure the progression of desirable environmental sensor based on the selective GST enzyme.

Table2 Surface profile exploration from AFM micrographs at 1x1 μm scan size of bare SPCE, SPCE-Chi, and SPCE-Chi-GST.

Analysis parameters	SPCE	SPCE-Chi	SPCE-Chi-GST
Ra (nm)	18.69	21.74	26.72
Rq (nm)	24.49	25.15	33.17
Rpv (nm)	157.23	111.62	143.38
Rz (nm)	155.24	108.88	142.81
Rsk	-0.19	-0.18	0.59
Rku	3.32	1.96	2.67
Rsm (μm)	0.39	0.11	0.09
Fractal (triangular)	2.14	2.27	2.02

Note: SPCE = screen printed carbon electrode, SPCE-Chi = chitosan modified screen printed carbon electrode, SPCE-Chi-GST = chitosan modified screen printed carbon electrode after immobilization with glutathione-s-transferase, Ra = roughness average, Rq = root mean square roughness or standard deviation of the height value, Rpv = peak-to-valley, Rz = ten point height, Rsk = skewness, Rku = kurtosis, Rsm = mean spacing average.

4. CONCLUSION

A fundamental step in enzyme biosensor development is to get success in the immobilization of a selected enzyme onto the suitable platform. In this study, an SPCE was chosen as a convenient basement for a self-assembled modification with biocompatible chitosan polymer, afterward, the enzyme GST was immobilized onto a working surface of this SPCE-Chi using glutaraldehyde as a crosslinker. To gain valuable information for a progressive achievement of immobilization, a nanoscale imaging and several analysis strategies via AFM were employed. The obtaining 3D AFM images have illustrated a clear distinction in morphological appearance among SPCE, SPCE-Chi, and SPCE-Chi-GST working surfaces. Statistical parameters and fractal geometry were used as two main analysis approach with an XEI software assistance for describing the surface roughness and complexity of irregular nanostructures. Determination of the surface grain size and distribution has denoted the asymmetric planar growth in grain area and a parameter of SPCE-Chi and SPCE-Chi-GST working surface. One of the most important parameters as power spectral density (PSD) curves were performed and proved capable to reflect differences among the roughness and its contribution on these surfaces. Fractal dimension character of each surface could be calculated with reference to this PSD function and an indicative value for diffusion-limited manner was gained from both SPCE-Chi and SPCE-Chi-GST as a result from surface modification with chitosan and subsequent immobilization with GST. Several other quantitative statistical parameters such as average roughness (Ra), root mean square roughness (Rq), peak-to-valley (Rpv), ten-point height (Rz), mean spacing average (Rsm), skewness (Rsk), kurtosis (Rku), and mean spacing average (Rsm) were also assessed. As summarized in Table1 and 2, all the worked out parameters indicate the complete layer by layer development in the SPCE-Chi and SPCE-Chi-GST. The outcome AFM images as well as surface topographical delineation of these prepared surfaces have revealed a surface dependent characteristic and consequently, a successfulness of the proposed simple direct self-assembling stepwise processing for well-done enzyme immobilization. Fabrication of desirable biosensor for real-time monitoring of specific environmental pollutants based on the selective GST enzyme shall be thus possible.

5. ACKNOWLEDGEMENTS

6. REFERENCES

[1] Wongkaew P, Poosittisak, S. "Diagnosis of sugarcane white leaf disease using the highly sensitive DNA based voltammetric electrochemical determination", Amer. J. of Plant Sciences, Vol. 5, Jul. 2014, pp. 2256-2268.

[2] Wongkaew P, Poosittisak, S."Atomic force microscopic and electrochemical characterization of the modified screen-printed carbon electrode by self-assembled deposition of chitosan and activated carbon" Int. J. of GEOMATE, Vol. 11, Aug.2016, pp. 2356-2362.

[3] Aminea A, Mohammadia H, Bourais I, Palleschi G, "Enzyme inhibition-based biosensors for food safetyand environmental monitoring" Biosens. Bioelectronics, Vol. 21, Mar. 2006, pp. 1405-1423.

[4] Vimala V, Clarke SK, UrvinderKaur S, "Pesticides detection using acetylcholinesterasenanobiosensor", Biosens. J., Vol. 5, Feb. 2016, pp.133.

[5] Brady D, Jordaan J, "Advances in enzyme immobilisation", Biotechnol. Letters, Vol. 11, Nov. 2009, pp. 1639-1650.

[6] Krajewska B, "Application of chitin- and chitosan-based materials for enzyme immobilizations: a review", Enzyme and Microbial Technology, Vol. 35, Aug. 2004, pp. 126–139.

[7] Singh RP, "Prospects of Organic Conducting PolymerModified Electrodes: Enzymosensors", Int. J. of Electrochemistry, Vol. 2012, Jan. 2012, pp. 1-14.

[8] Wongkaew P, Poosittisak, S, 2012. "Electro-affinity of SCWL-dsDNA on different high deacetylation degree chitosans deposited glassy carbon electrode", Advances in Developing Affordable In-Vitro Molecular Diagnostics, Puri CP, Abidi N, Bhanushali P, Pere A, Gupta SK, Eds., Yashraj Research Foundation, Varun Enterprises, 2012, pp. 249-258.

[9] Variola F, "Atomic force microscopy in biomaterials surface science", Phys. Chem. Chem. Physics, Vol. 17, Feb. 2015, pp. 2950-2959.

[10] Allocati N, Federici L, Masulli M, Di Ilio C, "Glutathione transferases in bacteria", FEBS Journal, Vol. 276, Jan. 2009, pp. 58–75.

[11] Yan F, Yang WK, Li XY, Lin TT, Lun YN, Lin F, Lv SW, Yan GL, Liu JQ, Shen JC, Mu Y, Luo G, "A trifunctional enzyme with glutathione S-transferase, glutathione peroxidase and superoxide dismutase activity", Biochim. Biophys. Acta., Vol. 1780, Jun. 2008, pp. 869-872.

[12] Singh RP, Kim YJ, Oh BK, Choi JW, "Glutathione-s-transferase based electrochemical biosensor for the detection of captan", Electrochem. Communications, Vol. 11, Jan. 2009, pp.181–185.

[13] Gavrila R, Dinescu A, Mardare D, "A power spectral density study of thin films morphology based on AFM profiling", Rom. J. Inform. Sci. Technology, Vol. 10, Sept. 2007, pp.291–300.

[14] Church EL, "Fractal surface finish", Appl. Optics, Vol. 27, Apr. 1988, pp. 1518-1526.

[15] Stach S, Cybo J, "Multifractal description of fracture morphology: theoretical basis", Mater. Characterization, Vol. 51, Aug. 2003, pp. 79-86.

[16] Ţălu S, Stach S, Ikram M, Pathak D, Wagner T, Nunzi J-M, "Surface roughness characterization of ZnO: TiO2-organic blended solar cells layers by atomic force microscopy and fractal analysis", Int. J Nanoscience, Vol. 13, Jun. 2014, No. 03, 12 pp.